Supporting Information

Baldwin et al. 10.1073/pnas.1423221112

SI Materials and Methods

Transgenic Mice. *Dectin-1* (1), *CARD9* (2), and *MyD88* (3) mutant mice on a C57BL/6 background were kindly provided by Tobias Hohl, Memorial Sloan Kettering Cancer Center, New York. *CR3* (*CD11b/CD18*) mutants (4), *TLR2* mutants, *CX3CR1*$^{GFP/+}$ reporter mice (5), and C57BL/6 WT controls (either CD45.1 or CD45.2) were purchased from The Jackson Laboratory. The mice were group-housed under a 12-h light/dark cycle with access to food and water ad libitum. Breeding pairs of *dectin-1; MyD88* compound mutant mice were kept on enrofloxacin-treated water [1.9 mL of Baytril injectable (22 mg/mL) per 250 mL water bottle] to compensate for severe immunodeficiency.

Preparation of PAMPs. Zymosan (6) and depleted zymosan (7) from *Saccharomyces cerevisiae* (InvivoGen) were suspended in PBS at a concentration of 12.5 μg/μL by incubating at 37 °C for 10 min and then vortexing. Aliquots were stored at 4 °C. LPS from *Escherichia coli* (Sigma-Aldrich) was dissolved in PBS (5 μg/μL). Curdlan, a particulate β(1, 3)-glucan and FDA-approved food additive (8) (Wako Chemicals), was obtained in powder form and was mechanically refined using a mortar and pestle continuously for 5 min, within 24 h before use. Immediately before use, refined curdlan was suspended at 25 μg/μL in sterile PBS by vortexing for 2 min. Immediately before eye injections, the solution was shaken vigorously to resuspend the curdlan. After the suspension was drawn up into a syringe, the syringe was visually inspected to ensure curdlan particles were present and that the needle had not been blocked by larger particles. The syringe was rinsed thoroughly with PBS after each injection.

ONC Surgery. Adult male and female mice (age 6–12 wk) were used for surgical procedures (9). The mice were anesthetized with 100 mg/kg ketamine and 10 mg/kg xylazine i.p.. The optic nerve was exposed through an incision in the conjunctiva and then compressed for 10 s with curved forceps (Dumont #5; Roboz) ∼1–2 mm behind the eye. Immediately after ONC, a Hamilton syringe with a 30 G removable needle was used for i.o. injections of ∼5 μL of PAMP, including zymosan (12.5 μg/μL in PBS), depleted zymosan (12.5 μg/μL in PBS), curdlan (25 μg/μL in PBS), ∼3 μL of LPS (5 μg/uL in PBS), or 5 μL of PBS.

After ONC and PAMP injection, the eyes were rinsed with a few drops of sterile PBS, and ophthalmic ointment (Puralube; Fera Pharmaceuticals) was applied on the operated eye. At 2 wk after surgery, mice were given a lethal dose of ketamine/xylazine i.p. and then perfused transcardially with PBS for 2 min, followed by ice-cold 4% paraformaldehyde in PBS for 5 min.

Histochemical Studies. For visualization of regenerating RGC axons, animals were perfused and optic nerves were dissected and postfixed in 4% paraformaldehyde in PBS overnight at 4 °C. For cryoprotection, nerves were transferred to a 30% sucrose/PBS solution and kept at 4 °C for at least 2 h and up to 2 wk (10). Optic nerves were imbedded in Tissue-Tek OCT Compound (Sakura Fintek USA, Inc.) and stored at −20 °C. Longitudinal sections (14 μm thick) were cut with a cryostat, mounted on Superfrost Plus microscope slides (Fisher Scientific), and stained with a sheep polyclonal anti-GAP43 antibody (9, 11). Alexa Fluor 488-conjugated donkey anti-sheep secondary antibody (Invitrogen) was used for fluorescent labeling.

For immunofluorescence labeling of the retina, eyes were dissected, postfixed as described above, cryoprotected, and sectioned at 25 μm. Sections were mounted on Superfrost Plus microscope slides and stained with anti–dectin-1 (Serotec) and anti-GFAP (eBiosciences) antibodies, followed by application of the appropriate Alexa Fluor-conjugated secondary antibody. Nuclear staining with DAPI (300 nM) was used to counterstain sections. Images were acquired using an Olympus IX71 inverted microscope attached to an Olympus DP72 digital camera.

Flow Cytometry. For the analysis of immune cells in the eye, mice were euthanized by isofluorane overdose at 7 d after ONC and perfused transcardially with PBS, after which the eyes were dissected and the vitreous fluid and retinae harvested. Retinae and vitreous fluid were pooled, homogenized, incubated in collagenase-D (1 mg/mL; Fisher Scientific) for 60 min at 37 °C, and rinsed in PBS before incubation with fluorochrome-conjugated antibodies (CD11b, CD45, CD45.1, CD45.2, CD11c, TLR2, Dectin-1, CD3, CD4, CD8, B220, NK1.1, and F4/80, all purchased from eBiosciences; Ly6C and Ly6G, purchased from Pharmingen). Dihydroethidium (Sigma-Aldrich) was added at a 0.1 mM concentration to stain cells for ROS production. The spleen was dissected, and splenocytes were passed through a 70-μm cell strainer. Red blood cells in spleen and blood were lysed with Ammonium-Chloride-Potassium (ACK) Lysing Buffer (Quality Biological). Flow cytometry was performed with a FACSCanto II cell analyzer (BD Biosciences). Cells were gated on forward and side scatter after doublet exclusion. Immune cells were identified as follows: monocytes/macrophages (CD45$^+$ CD11b$^+$ Ly6C$^+$ Ly6G$^-$), neutrophils (CD45$^+$ CD11b$^+$ Ly6C$^+$ Ly6G$^+$), DCs (CD45$^+$ CD11b$^+$ CD11c$^+$), B cells (CD45$^+$ CD11b$^-$ B220$^+$), T cells (CD45$^+$ CD11b$^-$ CD3$^+$ CD4$^+$ or CD8$^+$), NK cells (CD45$^+$ CD11b$^-$ NK1.1$^+$), and microglia (CD45^{low} CD11b$^+$ CX3CR1$^+$). All flow cytometry experiments were carried out with at least six mice (both eyes receiving the same treatment and pooled) per group, with the exception of *dectin-1*$^{-/-}$*; TLR2*$^{-/-}$ double-mutants (three mice).

Labeled Zymosan. At the time of ONC, Alexa Fluor 555-labeled zymosan (Life Technologies) was injected into one eye (5 μL, 12.5 μg/μL) of adult CX3CR1$^{+/GFP}$ mice. Animals were killed at 2, 6, and 18 h after ONC, and eyeballs were collected for flow cytometry analysis of retina-resident microglia and blood-derived neutrophils. Some retinae were cryosectioned and analyzed by confocal microscopy for the presence of GFP$^+$ microglia that had taken up Alexa Fluor 555-labeled zymosan particles.

Western Blot Analysis. To examine the activation of signaling pathways downstream of dectin-1, adult mice were subjected to ONC and i.o. injection of curdlan (5 μL, 25 μg/μL), PBS (5 μL), or LPS (3 μL, 5 μg/μL). After 6 h, mice were euthanized with CO_2, and eyes were extracted and snap-frozen in dry ice-cooled 2-methylbutane. Eyes were stored at −80 °C overnight. Lysates were prepared by homogenizing frozen eyes in ice-cold RIPA buffer (50 mM Tris·HCl pH 8.0, 150 mM NaCl, 0.1% SDS, 0.5% sodium deoxycholate, 1% Nonidet P-40) containing 50 mM beta-glycerophosphate and 100 μM sodium orthovanadate to inhibit phosphatases, and Sigma-Aldrich Protease Inhibitor Mixture (diluted 1:100). Nondissolved components were spun down at 18,000 × *g* for 5 min, after which supernatants were collected and the protein concentration of the supernatant was measured (BioRad BCA Kit).

Supernatants were combined with 2× Laemmli buffer, boiled for 10 min, separated by SDS/PAGE (40 μg of protein loaded

per lane), and transferred to PVDF membrane (Millipore). PVDF membranes were blocked with 2% milk (BioRad) in TBS-T (Tris-buffered saline pH 7.4, containing 0.1% Tween-20) and probed with antibodies specific for pERK (1:2,000; Cell Signaling), ERK (1:2,000; Cell Signaling), pSyk (1:1,000; Cell Signaling), Syk (1:1,000; Cell Signaling), pCREB (1:1,000; Upstate Biologicals), CREB (1:1,000; Cell Signaling), and β-actin (1:5,000; Sigma-Aldrich). Anti-mouse or anti-rabbit IgG-HRP (Millipore), along with West Pico Substrate or West Femto Substrate (Thermo Scientific), were used to detect primary antibodies.

Protein bands were visualized and quantified with LI-COR C-Digit and Image Studio software. Western blot band intensity in the linear range was measured with Image Studio software. For quantification, pERK levels were normalized to total ERK levels, pCREB levels were normalized to total CREB levels, and pSyk levels were normalized to total Syk and actin levels.

Generation of Dectin-1 BM Chimeras. Chimeric mice were generated as described previously (12). In brief, 5- to 6-wk-old recipient mice were lethally irradiated (13 Gy, split dose) and given congenic (CD45.1 or CD45.2) BM from donor mice (5 million cells in 300 μL) via tail vein injection. At 6 wk after BM transplant, ONC surgery was performed along with i.o. injection of ∼5 μL of curdlan (25 μg/μL) or PBS. One group of animals (26 mice total) was killed 14 d after ONC surgery. A second group of BM chimeric mice (21 mice total) was killed at 7 d after ONC surgery and i.o. injection of ∼5 μL of curdlan (25 μg/μL) or PBS. Nerves were isolated and assessed for RGC axon regeneration by anti-GAP43 labeling. Eyes were processed to assess the composition of the immune infiltrate by flow cytometry. Congenic markers (CD45.1 and CD45.2) were used to assess the degree of chimerism. All BM chimeras had >97% chimerism in the myeloid compartment.

Statistical Analysis. For quantification of RGC regeneration, GAP43$^+$ axons in optic nerve sections were counted at each 0.2-mm interval past the injury site up to 1.6 mm. For each nerve, at least three sections were quantified. The number of labeled axons per section was normalized to the width of the section and converted to the total number of regenerating axons per optic nerve, as described previously (11). All optic nerve data were analyzed by one-way ANOVA followed by Tukey's post hoc test using Graphpad Prism 6.0. The unpaired Student *t* test was used to analyze flow cytometry data with only two groups, and one-way ANOVA followed by Tukey's post hoc test was used to analyze flow cytometry data with more than two groups.

1. Saijo S, et al. (2007) Dectin-1 is required for host defense against *Pneumocystis carinii* but not against *Candida albicans*. *Nat Immunol* 8(1):39–46.
2. Hsu YM, et al. (2007) The adaptor protein CARD9 is required for innate immune responses to intracellular pathogens. *Nat Immunol* 8(2):198–205.
3. Adachi O, et al. (1998) Targeted disruption of the *MyD88* gene results in loss of IL-1– and IL-18–mediated function. *Immunity* 9(1):143–150.
4. Rosenkranz AR, et al. (1998) Impaired mast cell development and innate immunity in Mac-1 (CD11b/CD18, CR3)-deficient mice. *J Immunol* 161(12):6463–6467.
5. Mizutani M, et al. (2012) The fractalkine receptor, but not CCR2, is present on microglia from embryonic development throughout adulthood. *J Immunol* 188(1):29–36.
6. Di Carlo FJ, Fiore JV (1958) On the composition of zymosan. *Science* 127(3301):756–757.
7. Ikeda Y, et al. (2008) Dissociation of Toll-like receptor 2–mediated innate immune response to zymosan by organic solvent-treatment without loss of dectin-1 reactivity. *Biol Pharm Bull* 31(1):13–18.
8. Zhan XB, Lin CC, Zhang HT (2012) Recent advances in curdlan biosynthesis, biotechnological production, and applications. *Appl Microbiol Biotechnol* 93(2):525–531.
9. Dickendesher TL, et al. (2012) NgR1 and NgR3 are receptors for chondroitin sulfate proteoglycans. *Nat Neurosci* 15(5):703–712.
10. Winters JJ, et al. (2011) Congenital CNS hypomyelination in the Fig4 null mouse is rescued by neuronal expression of the PI(3,5)P(2) phosphatase Fig4. *J Neurosci* 31(48):17736–17751.
11. Leon S, Yin Y, Nguyen J, Irwin N, Benowitz LI (2000) Lens injury stimulates axon regeneration in the mature rat optic nerve. *J Neurosci* 20(12):4615–4626.
12. King IL, Kroenke MA, Segal BM (2010) GM-CSF–dependent, CD103$^+$ dermal dendritic cells play a critical role in Th effector cell differentiation after subcutaneous immunization. *J Exp Med* 207(5):953–961.

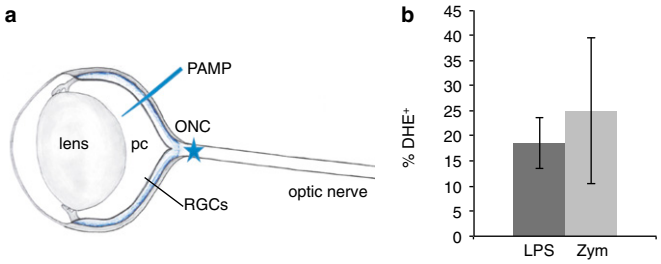

Fig. S1. Zymosan and LPS produce similar ROS levels in the eye. (*A*) Diagram of the mouse ONC injury model. The optic nerve is crushed at 1–2 mm behind the eyeball (ONC; asterisk). PAMPs are injected into the posterior chamber (pc) of the eye to elicit an inflammatory response near the cell soma of RGCs. (*B*) Adult WT mice were subjected to ONC and i.o. injection of LPS or zymosan. ROS production by macrophages was assessed by flow cytometry combined with dihyroethidium (DHE) staining at 7 d after ONC. The fraction of ROS-producing (DHE$^+$) cells was not significantly different in the LPS-injected and zymosan-injected eyes. Values represent the mean ± SEM for four mice in each group, from two independent sets of experiments.

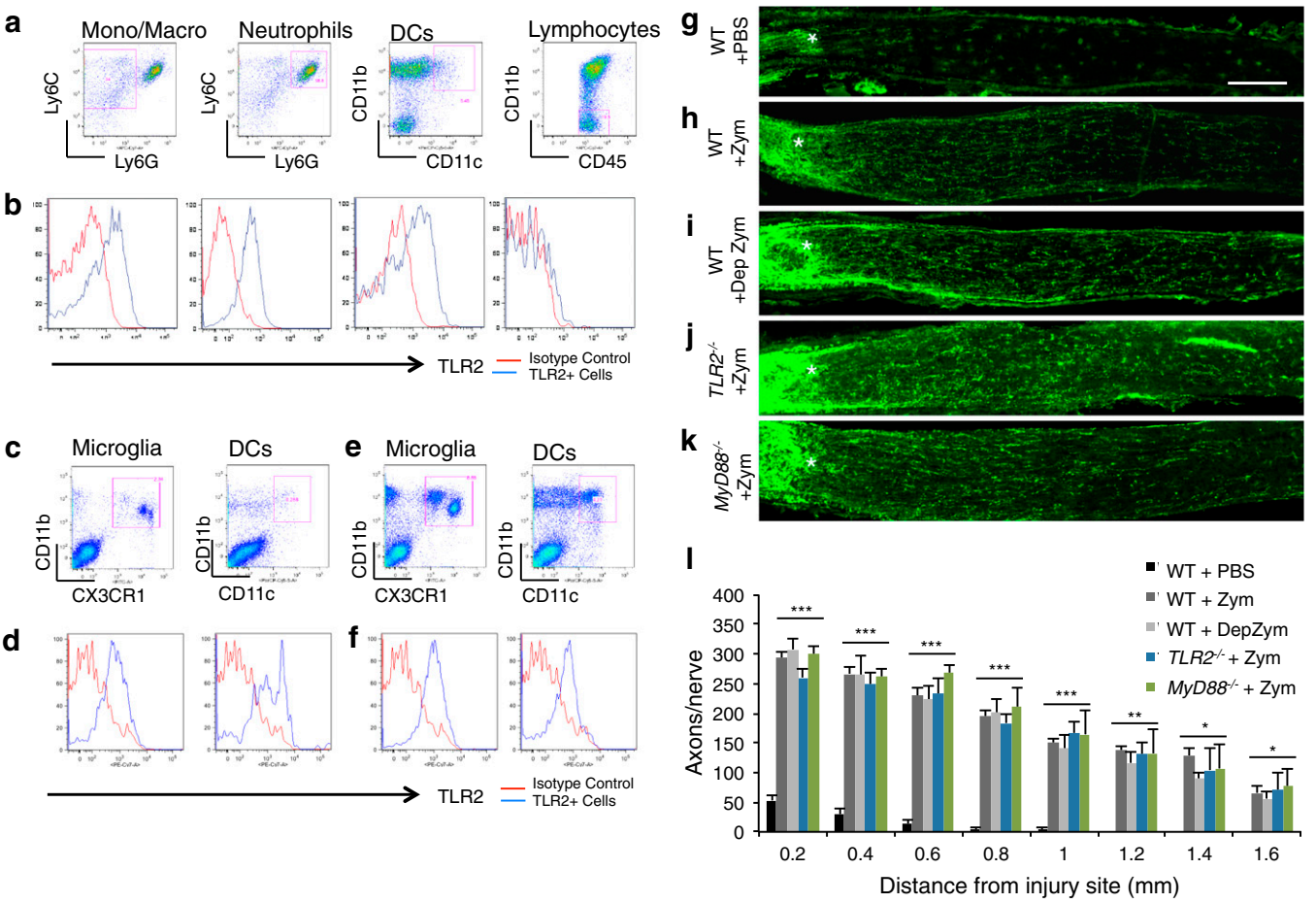

Fig. S2. TLR2 is expressed on retina-resident and blood-derived immune cells in the eye, but is not necessary for zymosan-induced RGC axon regeneration. (*A*) Flow cytometry analysis of immune cells accumulating in the eye at 7 d after ONC and i.o. zymosan injection. Shown are representative dot plots of monocytes/macrophages ($CD45^+/CD11b^+/Ly6C^+/LyG^-$), neutrophils ($CD45^+/CD11b^+/Ly6C^+/LyG^+$), DCs ($CD45^+/CD11b^+/CD11c^+$), and lymphocytes ($CD45^+/CD11b^-$). (*B*) Histograms representing TLR2 (blue) or isotype control (red) staining for the gated cell populations. (*C* and *D*) In the naïve retina, microglia ($CD45^+/CD11b^+/CX3CR1^+$) and DCs are present (*C*) and express TLR2 (*D*). (*E*) At 7 d post-ONC (without i.o. zymosan), cell counts increase from ~6,000 to ~24,000 for microglia and from ~700 to ~10,000 for DCs. (*F*) TLR2 expression on microglia and DCs at 7 d post-ONC. Plots and histograms are representative of two independent experiments. (*G*–*K*) Longitudinal sections of optic nerves at 14 d post-ONC stained with anti-GAP43. The injury site is marked with an asterisk. (Scale bar: 200 μm.) (*G*) WT mice receiving i.o. PBS (5 μL) at the time of injury show very little regenerative growth. (*H* and *I*) WT mice with i.o. zymosan (zym; 5 μL, 12.5 μg/μL) (*H*) or i.o. depleted zymosan (dep. zym; 5 μL, 12.5 μg/μL) (*I*) show robust RGC axon regeneration. (*J* and *K*) $TLR2^{-/-}$ mice with i.o. zymosan (*J*) and $MyD88^{-/-}$ mice with i.o. zymosan (*K*) show robust regeneration. (*L*) Quantification of the number of $GAP43^+$ axons per optic nerve at 0.2–1.6 mm distal to the injury site. WT + PBS, n = nerves and 5 mice; WT + zymosan, n = 6 nerves and 6 mice; WT + depleted zymosan, n = 4 nerves and 4 mice; $TLR2^{-/-}$ + zymosan, n = 4 nerves and 4 mice; $MyD88^{-/-}$ + zymosan, n = 4 nerves and 4 mice. Data are presented as mean ± SEM. Regeneration is significantly enhanced in all groups compared with WT + PBS. ***$P < 0.001$; **$P < 0.01$; *$P < 0.05$, one-way ANOVA, Tukey's post hoc test.

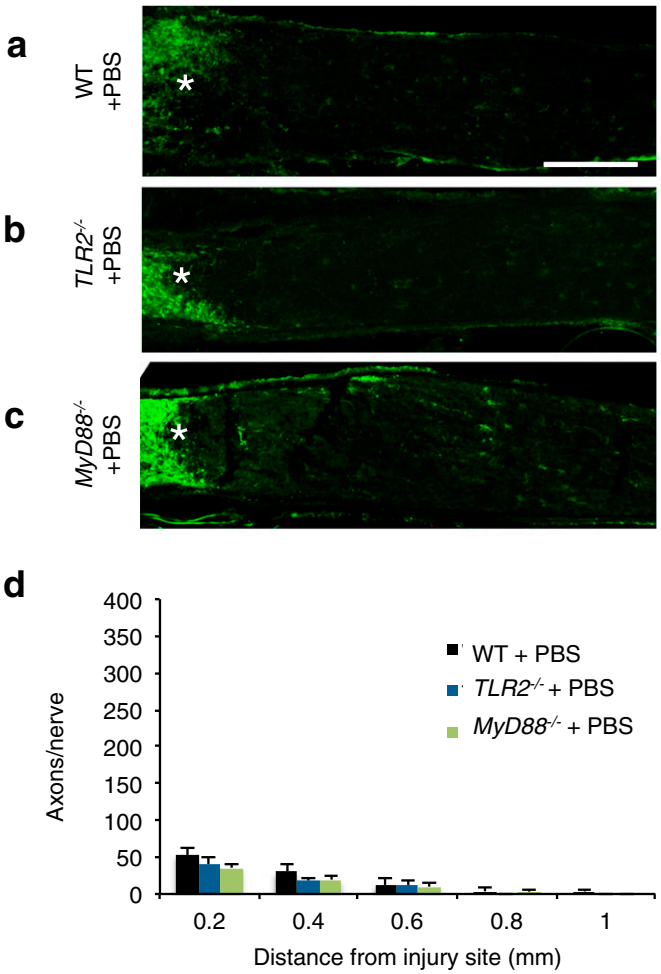

Fig. S3. Loss of *TLR2* or *MyD88* does not alter RGC axon regeneration. (*A*) WT mice with i.o. PBS (5 μL) show minimal RGC axon regeneration at 2 wk post-ONC, as assessed by anti-GAP43 staining of longitudinal optic nerve sections. The injury site in the nerve is marked with an asterisk. (Scale bar: 200 μm.) (*B* and *C*) Compared with WT mice, no significant difference in regeneration is observed in $TLR2^{-/-}$ mice ($n = 4$ nerves and 4 mice) (*B*) or $MyD88^{-/-}$ mice ($n = 3$ nerves and 3 mice) (*C*) subjected to i.o. PBS injection. (*D*) Quantification of $GAP43^{+}$ axons at 0.2–1.0 mm distal to the injury site. Results are presented as mean ± SEM number of axons per nerve.

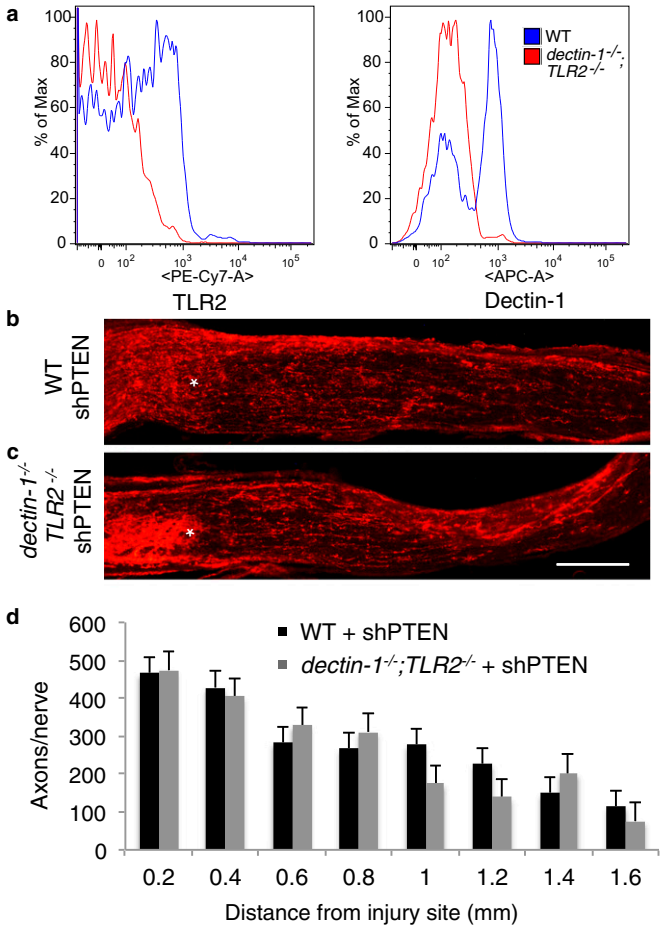

Fig. S4. Characterization of *dectin-1/TLR2* compound mutant mice. (*A*) As an independent confirmation that *dectin-1/TLR2* compound mutants are null for the PRRs dectin-1 and TLR2, we performed flow cytometry analysis of Ly6C^{+} myeloid cells isolated from the blood. Cells from double-mutant mice (red line) are negative for TLR2 and dectin-1. Cells from WT mice (blue line) express TLR2 and dectin-1 on their surface. (*B–D*) To verify that *dectin-1/TLR2* compound mutant mice are capable of RGC axon regeneration in a PAMP-independent context, PTEN expression in WT and *dectin-1/TLR2* mice was knocked down by i.o. injection of AAV2-shPTEN-GFP at 14 d before ONC (1). (*B*) Knockdown of *PTEN* elicits robust RGC axon regeneration in WT mice at 14 d after ONC, as assessed by anti-GAP43 staining. (*C*) Similarly robust RGC axon regeneration is observed in *dectin-1/TLR2* mutant mice after PTEN knockdown. (*D*) Quantification of the number of GAP43^{+} axons per nerve at 0.2–1.6 mm distal to the injury site. Results are presented as mean ± SEM from at least three nerves per condition.

1. Zukor K, et al. (2013) Short hairpin RNA against PTEN enhances regenerative growth of corticospinal tract axons after spinal cord injury. *J Neurosci* 33(39):15350–15361.

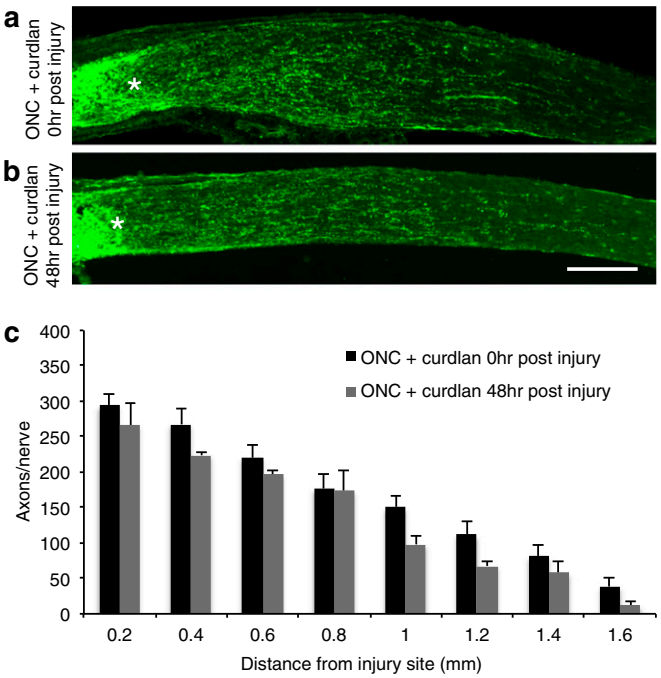

Fig. S5. Curdlan has a therapeutic window of at least 48 h. For assessment of the therapeutic window of i.o. curdlan-elicited RGC axon regeneration, ONC surgery was performed, and administration of curdlan was delayed for 2 d. (*A* and *B*) Longitudinal sections of mouse optic nerves at 2 wk after ONC injury. Regenerating axons are stained by anti-GAP43 immunofluorescence labeling. The injury site in the nerve is marked with an asterisk. (Scale bar: 200 μm.) Intraocular curdlan (5 μL, 25 μg/μL) was administered at 0 h (*A*) or 48 h (*B*) after ONC. Robust regeneration beyond the injury site was observed for both conditions. (*C*) Quantification of $GAP43^{+}$ axons at 0.2–1.6 mm distal to the injury site. Results are presented as mean ± SEM from at least four nerves per condition.

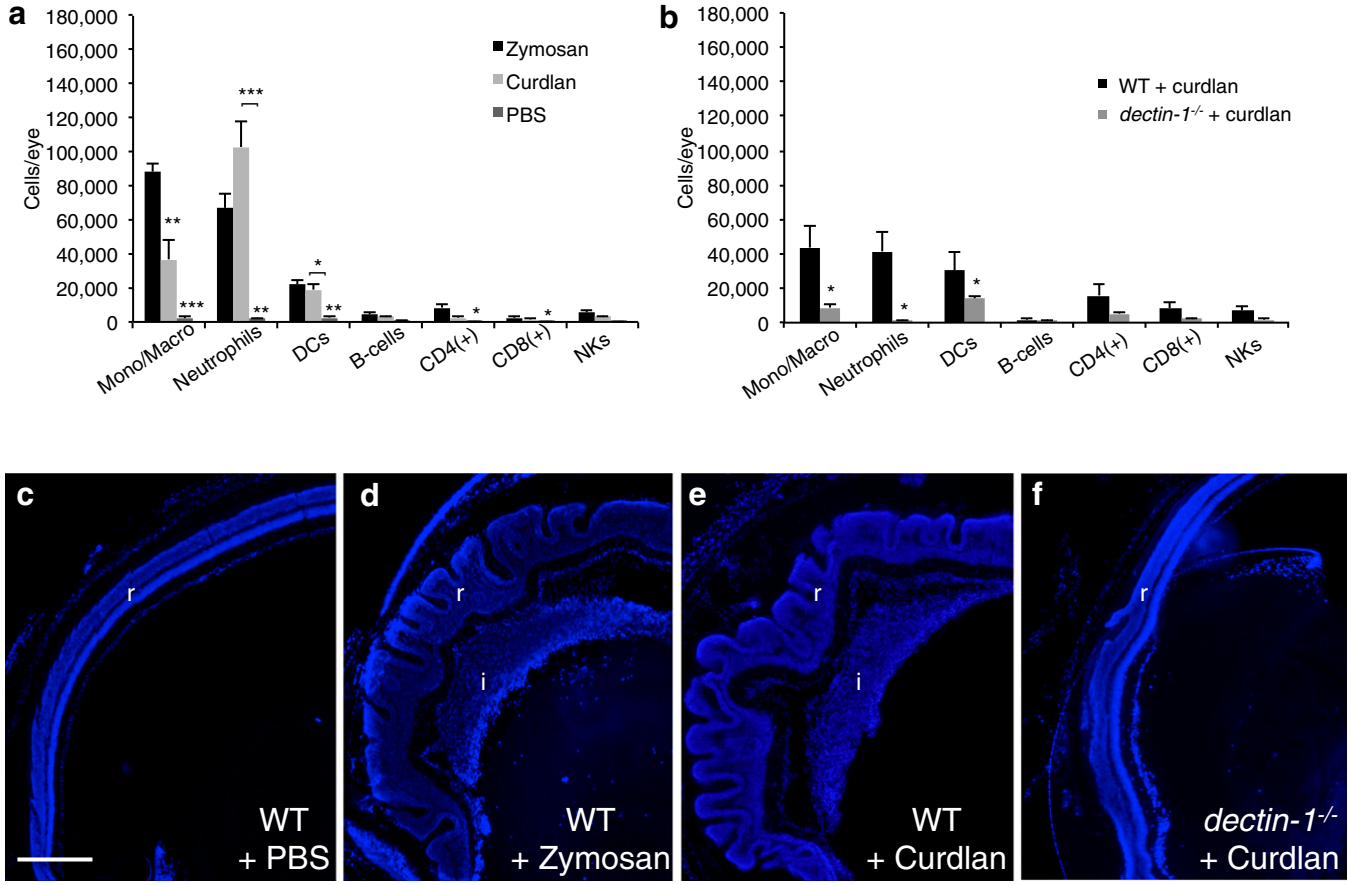

Fig. S6. Intraocular curdlan-elicited inflammation is associated with retinal damage. Flow cytometry analysis of immune cells accumulating in the eye at 7 d after ONC and i.o. PAMP injection. (*A*) Injection of zymosan (5 μL, 12.5 μg/μL; $n = 4$ mice) or curdlan (5 μL, 25 μg/μL; $n = 3$ mice) recruits monocytes/macrophages, neutrophils, DCs, and small numbers of B cells, $CD4^+$ T cells, $CD8^+$ T cells, and NK cells. With exception of the decreased number of monocytes/macrophages in curdlan-treated animals, the cellular composite is very comparable. Differences between zymosan- and curdlan-elicited inflammation likely reflect the fact that these two PAMPs use partially overlapping, yet distinct receptor mechanisms to trigger inflammation. In contrast to zymosan or curdlan, i.o. injection of PBS (5 μL; $n = 6$ mice) recruits few immune cells to the vitreous. For statistical analysis, the number of cells was compared with that in zymosan-injected eyes. Values are shown as mean ± SEM. $^{***}P < 0.001$; $^{**}P < 0.01$; $^{*}P < 0.05$, one-way ANOVA, Tukey's post hoc test. (*B*) Flow cytometry analysis of infiltrating immune cells in the eye at 7 d after ONC and i.o. curdlan injection. Compared with WT mice ($n = 12$ eyes), *dectin-1*$^{-/-}$ mice ($n = 12$ eyes) show significant reductions in the numbers of macrophages/monocytes (from 43,600 ± 12,000 to 8,800 ± 2,000), neutrophils (from 41,400 ± 11,100 to 1,300 ± 200), and DCs (from 19,000 ± 3,100 to 2,600 ± 500). The number of lymphocytes is not significantly altered. $^{*}P < 0.05$, unpaired Student *t* test. (*C*–*F*) Cross-sections of whole eyes stained with Hoechst at 14 d after ONC and i.o. injection of PBS, zymosan, or curdlan. The retina is labeled with an "r," and the accumulation of inflammatory cells in the vitreous is labeled with an "i." (Scale bar: 200 μm.) (*C*) The retinal morphology of WT mice with ONC and i.o. PBS appears largely normal after 14 d. (*D* and *E*) In contrast, i.o. zymosan (*D*) or i.o. curdlan (*E*) causes choroid detachment and extensive retinal folding. The accumulation of immune cells in the vitreous is clearly visible (indicated by "i"). (*F*) In marked contrast, i.o. curdlan does not induce noticeable retinal pathology in *dectin-1*$^{-/-}$ mice, indicating that dectin-1 activation underlies both the beneficial (proregenerative) and detrimental (toxic) aspects of i.o. inflammation.

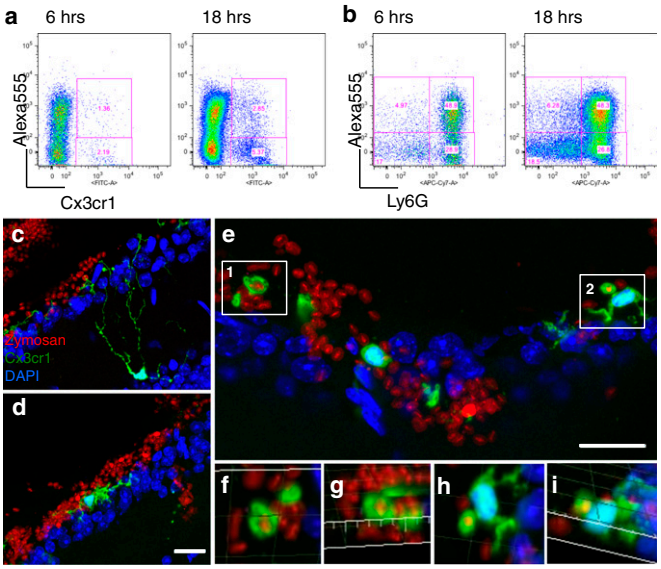

Fig. S7. Retina-resident microglia and infiltrating neutrophils rapidly phagocytose zymosan particles. (*A* and *B*) Alexa Fluor 555-conjugated zymosan particles were injected into the eye at the time of ONC, and zymosan-labeled cells were quantified by flow cytometry. (*A*) Dot plot of zymosan-labeled microglia at 6 h and 18 h after ONC and i.o. zymosan injection. At both time points, ∼40% of the CX3CR1^{+} microglia are positive for zymosan. (*B*) Ly6G^{+} neutrophils are abundant in the vitreous at both 6 h and 18 h after ONC and i.o. zymosan injection. Approximately 50% of neutrophils are positive for zymosan at both the 6 h and 18 h time points. Data are representative of at least two independent experiments. (*C*–*I*) Confocal images of retina of CX3CR1$^{GFP/+}$ reporter mice after ONC and i.o. injection of Alexa Fluor 555-conjugated zymosan. (Scale bar: 20 μm.) (*C* and *D*) At 2 h after zymosan injection, CX3CR1$^{GFP/+}$ microglia are highly branched, and phagocytosis of zymosan particles (red) is not observed. (*E*) At 6 h after zymosan injection, CX3CR1$^{GFP/+}$ microglia acquire a more rounded morphology and are positive for zymosan. (*F* and *G*) Confocal images of double-labeled cells (box 1 in *E*), rotated and magnified to show that zymosan particles are located within CX3CR1$^{GFP/+}$ microglia. (*H* and *I*) Rotated closeups of box 2, showing that zymosan particles are located within CX3CR1$^{GFP/+}$ microglia.

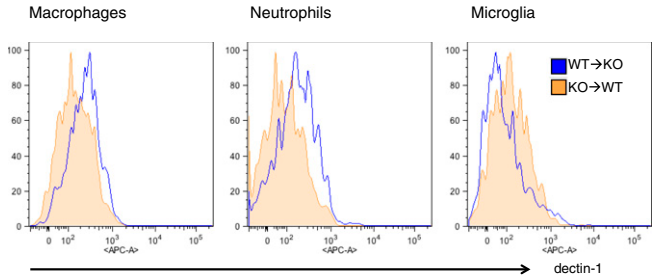

Fig. S8. BM chimeric mice are chimeric for dectin-1 expression. Flow cytometry was used to show that transplantation of WT BM into *dectin-1*$^{-/-}$ (KO) recipients [WT→KO] results in mice that express dectin-1 on blood-derived macrophages and neutrophils, but not on retina-resident microglia. Conversely, KO→WT chimeric mice lack dectin-1 on blood-derived immune cells, but express dectin-1 on retina-resident microglia.